

Supplementary information (SI)

Structure Engineering of MoO₃ Breaks the Scaling Relationship and Achieves High Electrocatalytic Oxygen Evolution Activity in Acid Conditions

Shuhua Wang, Zebin Ren, Shiqiang Yu, Baibiao Huang, Ying Dai,* and Wei Wei*
*School of Physics, State Key Laboratory of Crystal Materials, Shandong University,
Jinan 250100, China*

* Corresponding authors: daiy60@sdu.edu.cn (Y. Dai), weiw@sdu.edu.cn (W. Wei)

Details of the First-Principles Calculation

All calculations were performed based on the spin-polarized density functional theory in Vienna *ab initio* Simulation Package (VASP), employing projector-augmented wave method (PAW).¹⁻⁴ The exchange–correlation interactions were described by generalized gradient approximation (GGA) in form of Perdew–Burke–Ernzerhof (PBE) parameterization.^{5,6} The plane-wave cutoff energy of 520 eV was adopted. In the integration over the Brillouin zone, Monkhorst–Pack (MP) *k*-point grids of 3×3×1 and 5×5×1 were employed for geometry and electronic structures calculations, respectively. All structures were relaxed with the convergence criteria of 0.01 eV/Å and 10⁻⁵ eV for the maximal force on each atom and the energy, respectively. The U_{eff} (U_{eff} = Coulomb (U) – exchange (J)) values for considered transition metals (TMs) are summarized in Table S1. In the direction perpendicular to the material plane, a vacuum space was set to 20 Å to avoid the interactions between periodic slabs. In consideration of the van der

Waals (vdW) interaction, DFT–D3 correction proposed by Grimme was adopted.⁷ In addition, *ab initio* molecular dynamics (AIMD) simulations were carried out at 500 K for 5 ps with a time step of 1 fs for examining the thermal stability of MoO₃ monolayer.⁸ The phonon spectrum calculation was performed by using the PHONOPY code based on the finite-displacement method.⁹

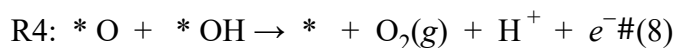
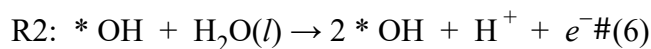
As an example, we examined Na adsorption on MoO₃ with different Na coverages (1/9, 2/9 and 1/3 monolayer (ML)). All the possible adsorption configurations and corresponding adsorption energies are summarized in Fig. S8 and Table S2, respectively. Results indicate that the Na adsorption energy varies slightly for all considered Na coverages. In addition, the effect of Na coverage on the OER overpotential of MoO₃ is verified to be also negligible, see Fig. S9. In this work, consequently, structure models based on a 3×3×1 supercell of MoO₃ with 1/9 ML AM coverage are used for optimization and further calculations, as shown in Fig. S10. In this case, substitutional TM doping corresponds to a doping ratio of 1.39%, as shown in Fig. S11.

Free Energy Change during the Oxygen Evolution Reaction (OER)

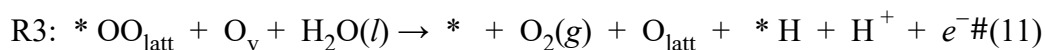
In acidic conditions, OER process involves four concerted proton–electron transfer (CPET) reactions for both adsorbate evolution mechanism (AEM) and lattice oxygen mechanism (LOM). The elementary steps for ER-type AEM are:



In case for the LH-type AEM, the elementary steps are:



The elementary steps for LOM are:



R4: $* \text{H} \rightarrow + \text{H}^+ + e^- \#(12)$ where $*$ represents the reaction site on the surface of catalysts; O_{v} means the remaining oxygen vacancy site after O_{latt} participating in the reactions; and $*\text{OH}$, $*\text{O}$, $*\text{OOH}$, $*\text{OO}_{\text{latt}}$ and $*\text{H}$ stand for the adsorbed intermediates at active sites.

The Gibbs free energy difference for elementary steps can be calculated based on the computational hydrogen electrode (CHE) model through the equation¹⁰

$$\Delta G = \Delta E + \Delta E_{\text{ZPE}} - T\Delta S + \Delta G_{\text{U}} \#(13)$$

where ΔE is the reaction energy defined as the energy difference between the reactant and product adsorbed on the catalyst surface, which can be obtained from the first-principles calculation; ΔE_{ZPE} and ΔS are the changes of zero-point energy and entropy, respectively; $\Delta G_{\text{U}} = -neU$ with U and n being the applied electrode potential and the number of electrons transferred, respectively.

Oxygen Vacancy Formation Energy

The formation energy of oxygen vacancy is defined as

$$E_f^{O_v} = E_{O_v} - (E_0 - 0.5E_{O_2}) \quad (14)$$

where E_{O_v} , E_0 and E_{O_2} represent the total energy of MoO₃ with oxygen vacancy, pristine MoO₃ monolayer and the energy of a free O₂ molecule, respectively.

Table S1 Hubbard U values for the transition metals. The unit is eV.

Element	Fe	Co	Ni	Mo	Ru	Ir
Hubbard U	4 (ref. 11)	3.3 (ref. 11)	5 (ref. 12)	6.3 (ref. 13)	2 (ref. 14)	2 (ref. 15)

Table S2 Na adsorption energy (E_{ad}) and relative adsorption energy (ΔE_{ad} , taking $\text{MoO}_3(\text{Na})$ as energy reference) for various adsorption configurations and Na coverages. The unit is eV.

Coverage	Configurations	E_{ad}	ΔE_{ad}
1/9 ML	$\text{MoO}_3(\text{Na})$	-3.56	0
2/9 ML	$\text{MoO}_3(2\text{Na})\text{-S1}$	-3.53	0.03
	$\text{MoO}_3(2\text{Na})\text{-S2}$	-3.49	0.07
	$\text{MoO}_3(2\text{Na})\text{-S3}$	-3.49	0.07
1/3 ML	$\text{MoO}_3(3\text{Na})\text{-S1}$	-3.45	0.11
	$\text{MoO}_3(3\text{Na})\text{-S2}$	-3.49	0.07
	$\text{MoO}_3(3\text{Na})\text{-S3}$	-3.53	0.03
	$\text{MoO}_3(3\text{Na})\text{-S4}$	-3.49	0.07

Table S3 Overpotentials for OER along different reaction pathways on various MoO₃ systems. The unit is V.

System	AEM	LOM-O ₁	LOM-O ₃
MoO ₃	1.84	1.84	1.84
MoO ₃ -Ov	2.14	0.67	1.67
MoO ₃ (Li)	0.45	0.50	1.29
MoO ₃ (Na)	0.44	0.60	1.38
MoO ₃ (K)	0.47	0.62	1.26
MoO ₃ (Cs)	0.52	0.66	1.23
System	AEM(ER)	AEM(LH)	LOM
MoO ₃ -Ov(Li)	2.09	–	2.08
MoO ₃ -Ov(Na)	1.93	–	2.02
MoO ₃ -Ov(K)	2.19	–	2.09
MoO ₃ -Ov(Cs)	2.16	–	2.06
Fe-MoO ₃	0.71	–	0.44
Co-MoO ₃	0.42	–	0.29
Ni-MoO ₃	1.05	–	1.05
Ru-MoO ₃	0.80	–	1.13
Ir-MoO ₃	0.77	–	0.96
Fe-MoO ₃ (Na)	0.33	–	0.33
Co-MoO ₃ (Na)	0.24	–	0.19
Ni-MoO ₃ (Na)	0.71	–	0.69
Ru-MoO ₃ (Na)	0.77	–	1.16
Ir-MoO ₃ (Na)	0.92	–	1.07

Table S4 Band center of $O_{\text{latt}}-p$ ($O_{\text{latt}}-\varepsilon_p$) and $\text{TM}-d$ ($\text{TM}-\varepsilon_d$) states in $\text{TM}-\text{MoO}_3$ and $\text{TM}-\text{MoO}_3(\text{Na})$ systems. The unit is eV.

System	$O_{\text{latt}}-\varepsilon_p$	$\text{TM}-\varepsilon_d$
Fe-MoO ₃	-1.43	-2.26
Co-MoO ₃	-1.55	-2.08
Ni-MoO ₃	-1.85	-3.08
Ru-MoO ₃	-1.52	-1.86
Ir-MoO ₃	-2.06	-2.13
Fe-MoO ₃ (Na)	-0.76	-1.91
Co-MoO ₃ (Na)	-1.33	-1.82
Ni-MoO ₃ (Na)	-1.60	-2.84
Ru-MoO ₃ (Na)	-1.98	-1.50
Ir-MoO ₃ (Na)	-2.24	-2.06

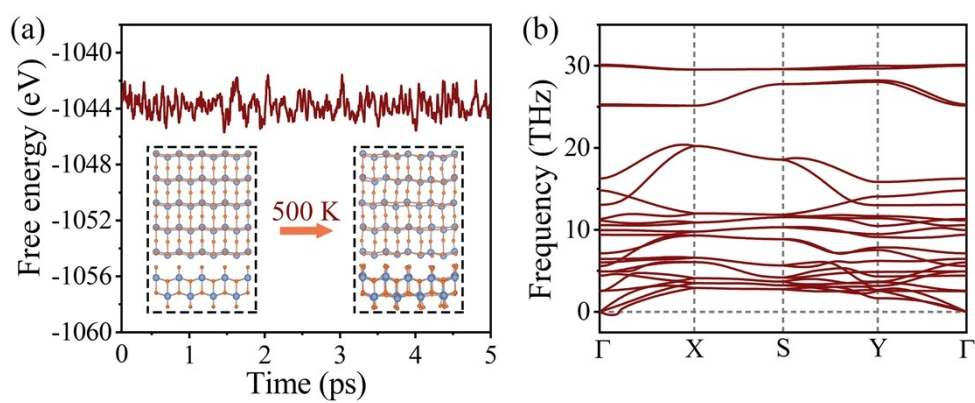


Fig. S1 (a) Ab initio molecular dynamics (AIMD) simulation results and (b) phonon spectrum of MoO₃ monolayer.

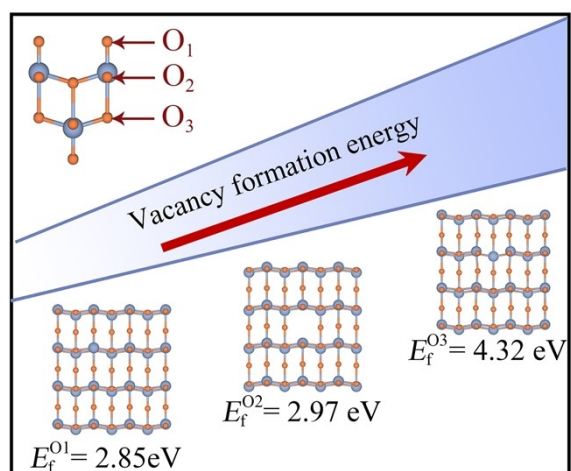


Fig. S2 Formation energy of oxygen vacancy in MoO₃ monolayer at various positions.

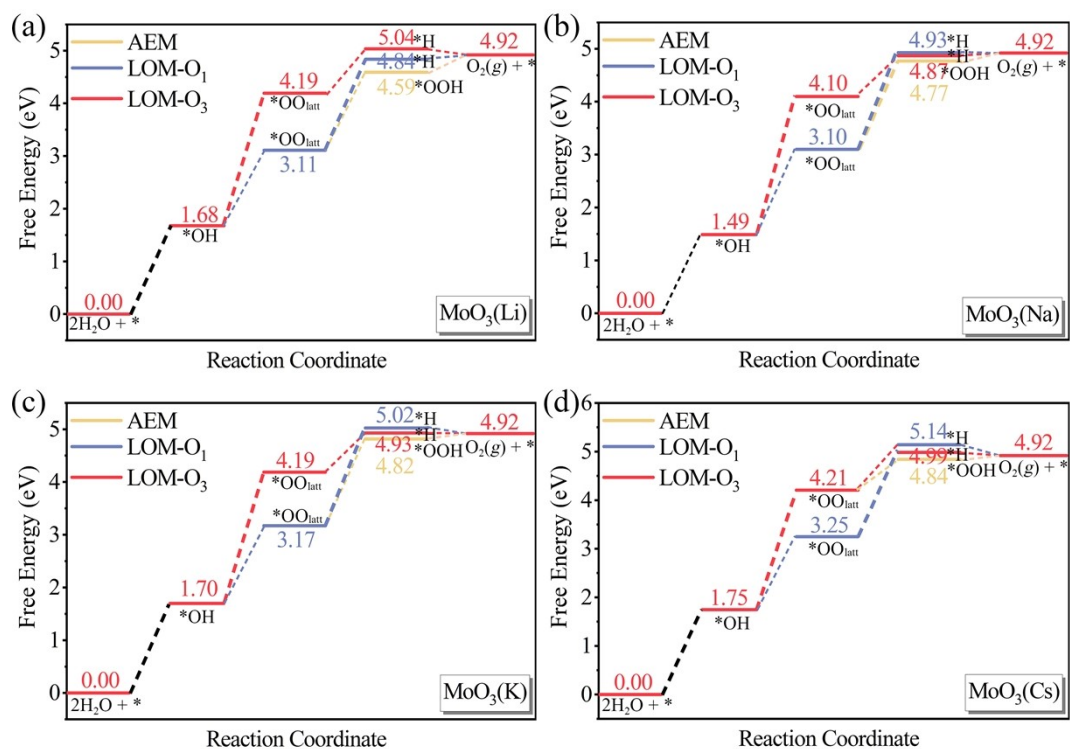


Fig. S3 Gibbs free energy diagrams of OER along different pathways on $\text{MoO}_3(\text{AM})$ with AM being (a) Li, (b) Na, (c) K and (d) Cs.

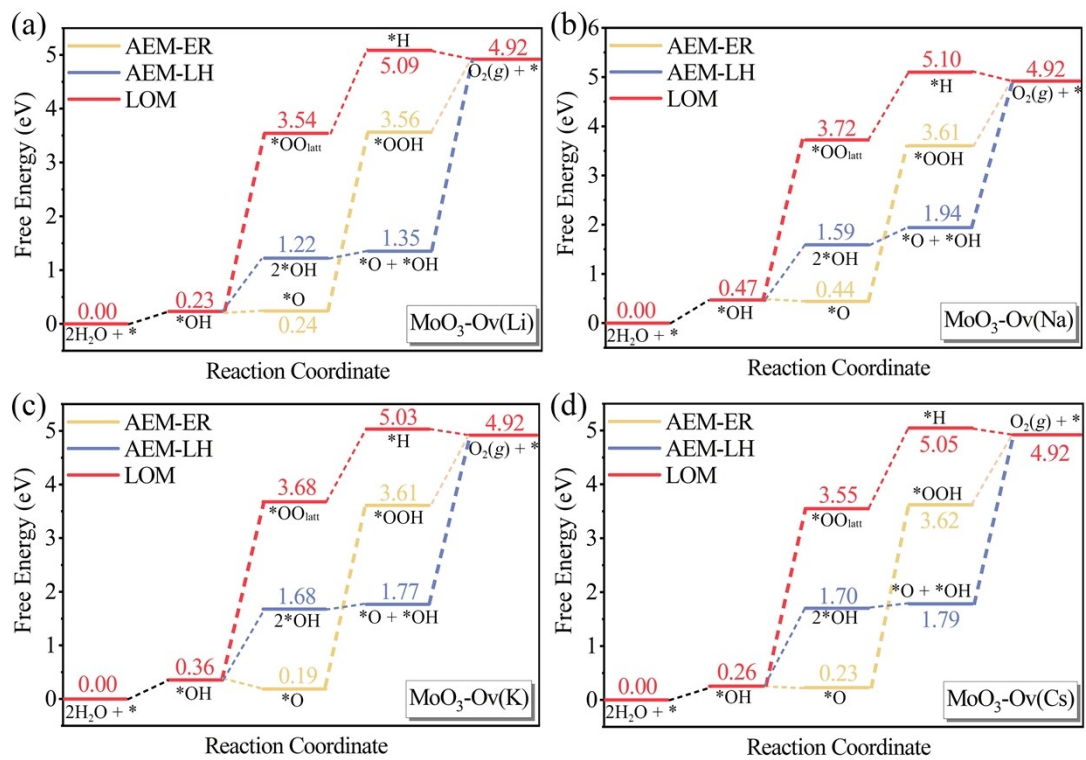


Fig. S4 Gibbs free energy diagrams of OER along different pathways on $\text{MoO}_3\text{-Ov}(\text{AM})$ with AM being (a) Li, (b) Na, (c) K and (d) Cs.

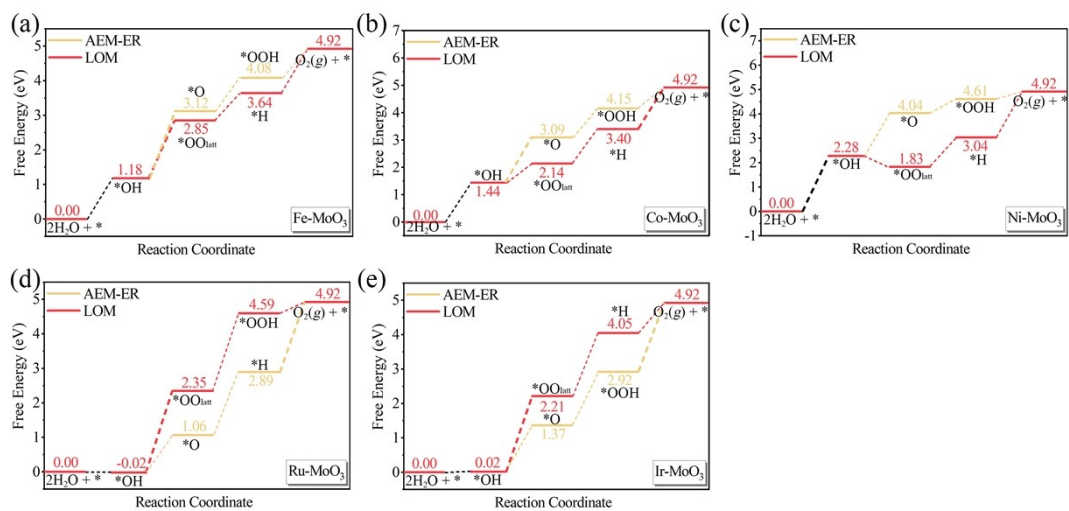


Fig. S5 Gibbs free energy diagrams of OER along different pathways on (a) Fe-, (b) Co-, (c) Ni-, (d) Ru- and (e) Ir-MoO₃.

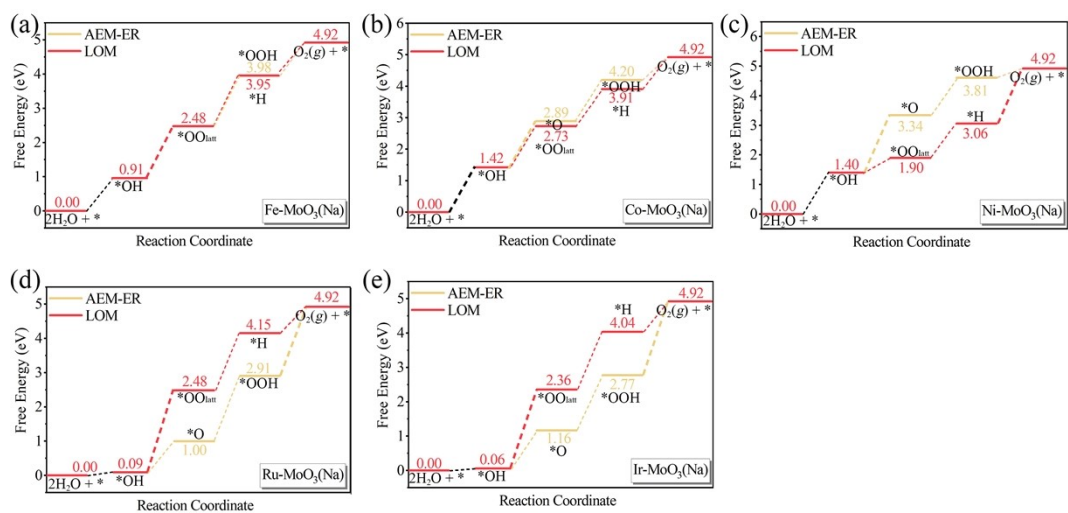


Fig. S6 Gibbs free energy diagrams of OER along different pathways on (a) Fe-, (b) Co-, (c) Ni-, (d) Ru- and (e) Ir-MoO₃(Na).

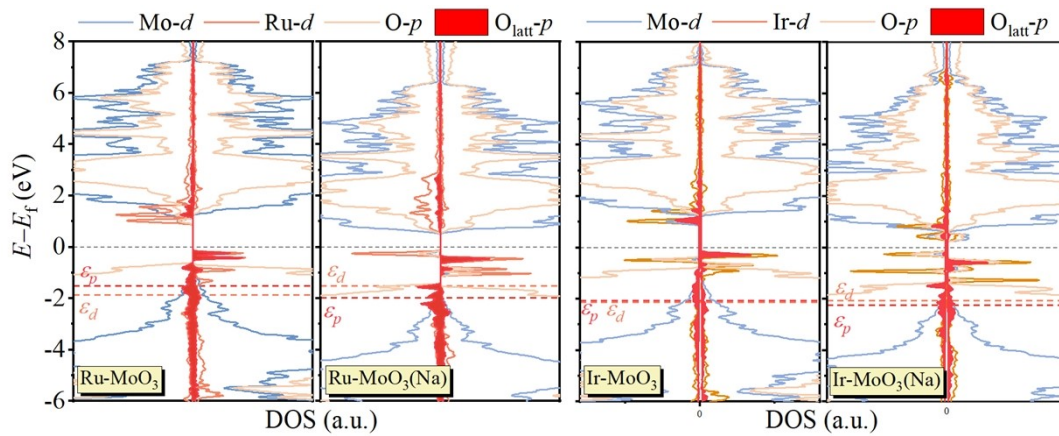


Fig. S7 Projected density of states (DOS) of $O-p$, $O_{\text{latt}}-p$ and $(\text{Mo}, \text{Ru}, \text{Ir})-d$ orbitals for $(\text{Ru}, \text{Ir})-\text{MoO}_3$ and $(\text{Ru}, \text{Ir})-\text{MoO}_3(\text{Na})$. The Fermi level is set to zero.

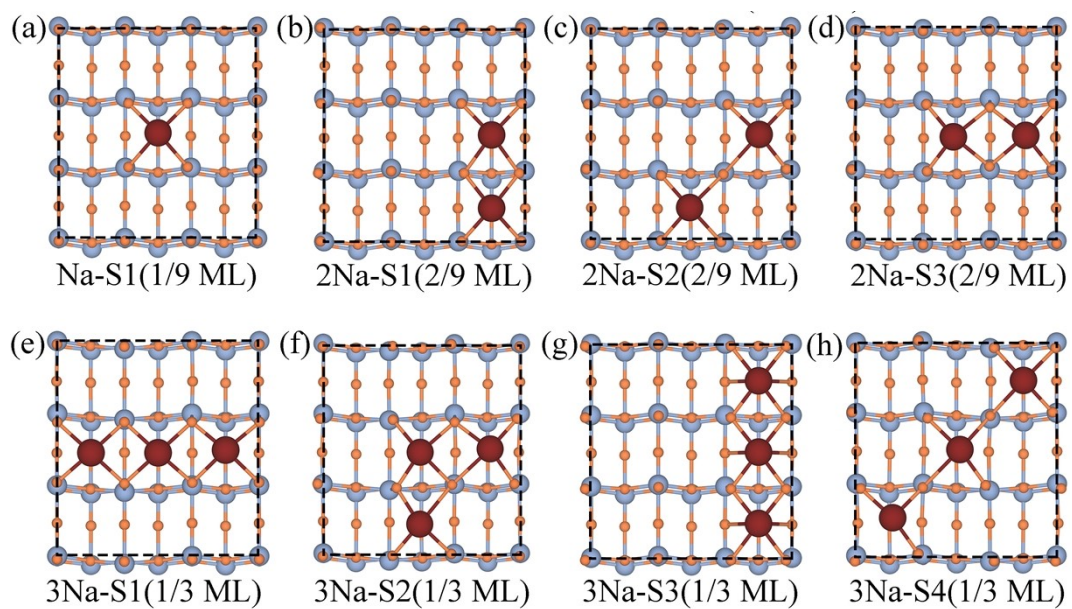


Fig. S8 Na adsorption configuration with Na coverage being (a) 1/9 ML, (b)–(d) 2/9 ML and (e)–(h) 1/3 ML.

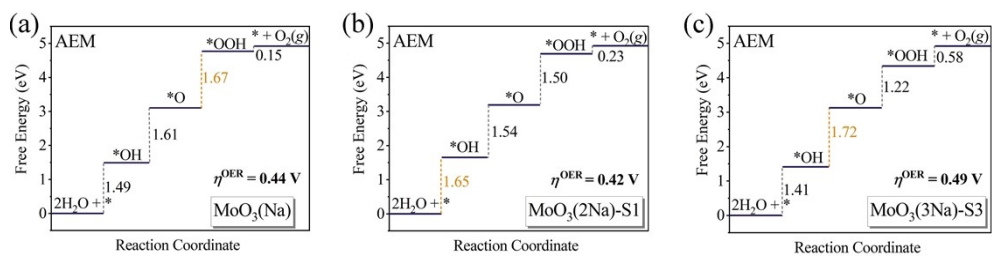


Fig. S9 Gibbs free energy diagrams of OER following AEM on MoO_3 with different Na coverage. (a) 1/9 ML, (b) 2/9 ML, and (c) 1/3 ML.

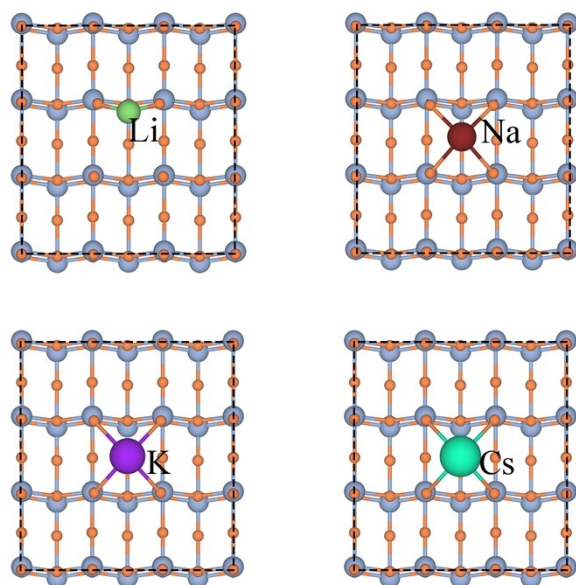


Fig. S10 Computational supercells of $\text{MoO}_3(\text{AM})$ (AM = Li, Na, K and Cs).

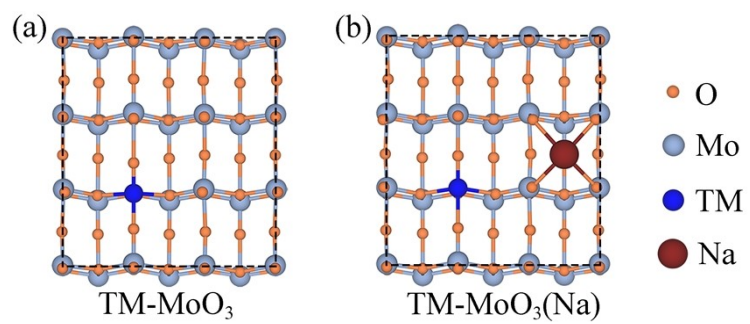


Fig. S11 Computational supercells of (a) TM-MoO₃ and (b) TM-MoO₃(Na).

References

- 1 G. Kresse and J. Furthmuller, *J. Comp. Mater. Sci.*, 1996, **6**, 15–50.
- 2 G. Kresse and J. Furthermüller, *Phys. Rev. B*, 1996, **54**, 11169.
- 3 P. E. Blöchl, *Phys. Rev. B*, 1994, **50**, 17953.
- 4 G. Kresse and D. Joubert, *Phys. Rev. B*, 1999, **59**, 1758.
- 5 J. P. Perdew, M. Ernzerhof and K. Burke, *J. Chem. Phys.*, 1996, **105**, 9982–9985.
- 6 J. P. Perdew, K. Burke and M. Ernzerhof, *Phys. Rev. Lett.*, 1996, **77**, 3865.
- 7 S. Grimme, *J. Comput. Chem.* 2006, **27**, 1787–1799.
- 8 R. N. Barnett and U. Landman, *Phys. Rev. B* 1993, **48**, 2081.
- 9 A. Togo and I. Tanaka, *Scr. Mater.* 2015, **108**, 1–5.
- 10 J. K. Nørskov, T. Bligaard, A. Logadottir, J. R. Kitchin, J. G. Chen, S. Pandalov and U. Stimming, *J. Electrochem. Soc.*, 2005, **152**, 23–26.
- 11 L. Wang, T. Maxisch and G. Ceder, *Phys. Rev. B*, 2006, **73**, 195107.
- 12 O. Bengone, M. Alouani, M. Blöchl and J. Hugel, *Phys. Rev. B*, 2000, **62**, 16392.
- 13 R. Coquet and D. J. Willock, *Phys. Chem. Chem. Phys.*, 2005, **7**, 3819.
- 14 A. Chikamatsu, Y. Kurauchi, K. Kawahara, O. Tomoya, M. Minohara, H. Kumigashira, E. Ikenaga and T. Hasegawa, *Phys. Rev. B*, 2018, **97**, 235101.
- 15 J. Liu, J. Xiao, Z. Wang, H. Yuan, Z. Lu, B. Luo, E. Tian and G. I. N. Waterhouse, *ACS Catal.*, 2021, **11**, 5386–5395.